Lecture 8: BAO, RSD, and the AP Effect (II)

Gong-Bo Zhao

Abstract

This lecture develops the equations behind anisotropic galaxy clustering. We derive the linear redshift-space distortion formula, explain the Kaiser effect and the Fingers-of-God effect, and then revisit the Alcock-Paczynski mapping in a form suitable for practical data analysis.

Learning goals

After this lecture, students should be able to:

- write the mapping from real-space position to redshift-space position;
- derive the linear Kaiser formula and interpret the parameter $\beta = f/b$;
- distinguish large-scale Kaiser squashing from small-scale Fingers-of-God;
- understand how AP scaling parameters distort transverse and radial modes differently;
- outline the logic of an anisotropic clustering fit.

1 From real space to redshift space

Let $\mathbf{r}$ be the true comoving position of a galaxy and let $v_\parallel$ be its peculiar velocity along the line of sight $\hat{\mathbf{n}}$. To first order, the inferred redshift-space position is

$$\mathbf{s} = \mathbf{r} + \frac{v_\parallel}{aH}\,\hat{\mathbf{n}}.$$

So only the line-of-sight coordinate is shifted. This is why the distortion is anisotropic.

For small peculiar velocities,

$$1 + z_{\rm obs} \approx (1 + z_{\rm cos}) \left(1 + \frac{v_\parallel}{c}\right),$$

which shows directly how Doppler shifts perturb the redshift we observe.

2 Mass conservation and the Jacobian

Galaxy number is conserved under the mapping from $\mathbf{r}$ to $\mathbf{s}$:

$$[1 + \delta^s(\mathbf{s})]\mathrm{d}^3 s = [1 + \delta(\mathbf{r})]\mathrm{d}^3 r.$$

Therefore the redshift-space overdensity is determined by the Jacobian of the transformation. In linear theory this leads to a correction proportional to the velocity gradient along the line of sight.

3 Linear redshift-space distortion

Using the continuity equation, the velocity divergence is related to the matter density contrast. In Fourier space, linear theory gives

$$\delta^s(\mathbf{k}) = \delta(\mathbf{k}) + f\mu^2\,\delta(\mathbf{k}) = \left(1 + f\mu^2\right)\delta(\mathbf{k}),$$

where

$$\mu \equiv \frac{k_\parallel}{k}, \qquad f \equiv \frac{\mathrm{d}\ln D}{\mathrm{d}\ln a}$$

is the linear growth rate.

If galaxies are biased tracers of matter with $\delta_g = b\,\delta_m$, then

$$\delta_g^s(\mathbf{k}) = \left(b + f\mu^2\right)\delta_m(\mathbf{k}) = b\left(1 + \beta\mu^2\right)\delta_m(\mathbf{k}),$$

with

$$\beta \equiv \frac{f}{b}.$$

4 The Kaiser formula

Squaring the previous expression gives the linear redshift-space galaxy power spectrum:

$$P_g^s(k,\mu) = \left(b + f\mu^2\right)^2 P_m(k) = b^2\left(1 + \beta\mu^2\right)^2 P_m(k).$$

This is the Kaiser formula. It describes the large-scale anisotropy produced by coherent infall.

Power-spectrum multipoles. Expanding in Legendre polynomials,

$$P_g^s(k,\mu) = \sum_\ell P_\ell(k)\,\mathcal{L}_\ell(\mu),$$

the first three nonzero multipoles in linear theory are

$$P_0(k) = b^2\left(1 + \frac{2\beta}{3} + \frac{\beta^2}{5}\right)P_m(k),$$

$$P_2(k) = b^2\left(\frac{4\beta}{3} + \frac{4\beta^2}{7}\right)P_m(k),$$

$$P_4(k) = b^2\left(\frac{8\beta^2}{35}\right)P_m(k).$$

These relations are useful because the ratio of multipoles can be used to constrain β and hence the growth rate.

5 The Fingers-of-God effect

On small scales, galaxies inside virialized halos have large random velocities. This produces a very different anisotropy: structures become stretched along the line of sight in redshift space. This is called the Fingers-of-God effect.

So there are two qualitatively different RSD regimes:

- **large-scale Kaiser effect:** coherent infall, usually appearing as squashing;
- **small-scale Fingers-of-God:** random virial motions, usually appearing as elongation.

In phenomenological models, small-scale damping is often described by a factor such as

$$D_{\mathrm{FOG}}(k\mu\sigma_v),$$

with Gaussian or Lorentzian forms.

6 AP revisited

If the true cosmology differs from the fiducial one used to build the catalog, radial and transverse distances are scaled differently:

$$s_\perp^{\rm fid} = \alpha_\perp \, s_\perp, \qquad s_\parallel^{\rm fid} = \alpha_\parallel \, s_\parallel.$$

In Fourier space the inverse scaling applies:

$$k_\perp = \frac{k_\perp^{\rm fid}}{\alpha_\perp}, \qquad k_\parallel = \frac{k_\parallel^{\rm fid}}{\alpha_\parallel}.$$

The power spectrum transforms as

$$P^{\rm fid}(k^{\rm fid}, \mu^{\rm fid}) = \frac{1}{\alpha_\perp^2 \alpha_\parallel} P^{\rm true}(k, \mu).$$

It is also convenient to define the anisotropy parameter

$$F_{\rm AP} \equiv \frac{\alpha_\parallel}{\alpha_\perp}.$$

7 Why AP and RSD are mixed in real data

In observations, AP and RSD both create anisotropy in the same two-dimensional clustering pattern. That is why realistic analyses fit them simultaneously. Roughly speaking:

- AP changes geometry;
- RSD changes dynamics;
- BAO adds a preferred ruler that helps break degeneracies.

8 A practical fitting strategy

A simplified anisotropic clustering analysis usually follows these steps:

1. build the galaxy catalog and a matching random catalog;
2. measure $\xi(s, \mu)$ or the power-spectrum multipoles;
3. model BAO, RSD, and AP together;
4. fit for quantities such as D_M/r_s, Hr_s, and $f\sigma_8$;
5. compare the results with cosmological models.

9 Detailed derivations and observational examples

This section collects a more explicit set of derivations and observational examples, complementing the main 2026 presentation.

9.1 More exact mapping between observed redshift and redshift-space position

One may write [3]

$$1 + z_{\rm obs} = (1 + z_{\rm cos}) \left(1 - \frac{v_\parallel(\boldsymbol{r})}{c}\right)^{-1},$$

so that the inferred position in redshift space is

$$\boldsymbol{s} = \boldsymbol{r} + \frac{(1 + z_{\rm cos}) v_\parallel(\boldsymbol{r})}{H(z_{\rm cos})}\,\hat{\boldsymbol{r}}.$$

Number conservation implies

$$\rho^s_{\rm m}(\boldsymbol{s})\,{\rm d}\boldsymbol{s} = \rho_{\rm m}(\boldsymbol{r})\,{\rm d}\boldsymbol{r}.$$

The Jacobian is therefore

$$J \equiv \left|\frac{{\rm d}\boldsymbol{r}}{{\rm d}\boldsymbol{s}}\right| = \frac{r^2\,{\rm d}r}{s^2\,{\rm d}s} = \left\{1 - \frac{1 + z_{\rm cos}}{H(z_{\rm cos})}\frac{v_\parallel}{r}\right\}^{-2} \left\{1 - \frac{1 + z_{\rm cos}}{H(z_{\rm cos})}\frac{\partial v_\parallel}{\partial r}\right\}^{-1}.$$

In the distant-observer or linearized limit, this becomes

$$J \simeq \left\{1 - \frac{1 + z_{\rm cos}}{H(z_{\rm cos})}\frac{\partial v_\parallel}{\partial r}\right\}^{-1}.$$

9.2 Velocity divergence and the linear Kaiser limit

Define the velocity-divergence field by

$$\theta(\boldsymbol{x}) \equiv -\frac{\nabla \cdot \boldsymbol{v}(\boldsymbol{x})}{aHf}.$$

In Fourier space,

$$\boldsymbol{v}(\boldsymbol{k}) = -iaHf\frac{\boldsymbol{k}}{k^2}\theta(\boldsymbol{k}).$$

The redshift-space density contrast can be written as

$$\delta^s_{\rm m}(\boldsymbol{s}) = \left|\frac{{\rm d}\boldsymbol{s}}{{\rm d}\boldsymbol{r}}\right|^{-1} [1 + \delta_{\rm m}(\boldsymbol{r})] - 1,$$

and, keeping the line-of-sight direction as the z-axis,

$$\delta^s_{\rm m}(\boldsymbol{k}) = \int {\rm d}^3x \left\{\delta_{\rm m}(\boldsymbol{x}) - \frac{1}{aH}\frac{\partial v_z(\boldsymbol{x})}{\partial z}\right\} \exp\left[i\boldsymbol{k}\cdot\boldsymbol{x} + i\frac{k\mu v_z}{aH}\right].$$

At linear order,

$$\delta^{s,L}_{\rm m}(\boldsymbol{k}) = \delta_{\rm m}(\boldsymbol{k}) + f\mu^2\theta(\boldsymbol{k}) = \left(1 + f\mu^2\right)\delta^L_{\rm m}(\boldsymbol{k}),$$

where in the last step we used $\theta = \delta$ in linear theory. This reproduces the Kaiser result

$$P^s_g(k,\mu) = (b + f\mu^2)^2 P_m(k).$$

For an early observational application, see Peacock et al. [4].

9.3 Observed anisotropy in configuration space

Figure 1 shows the anisotropic two-dimensional correlation function measured from BOSS galaxies [5]. The large-scale squashing and the small-scale line-of-sight stretching are the classic signatures of RSD.

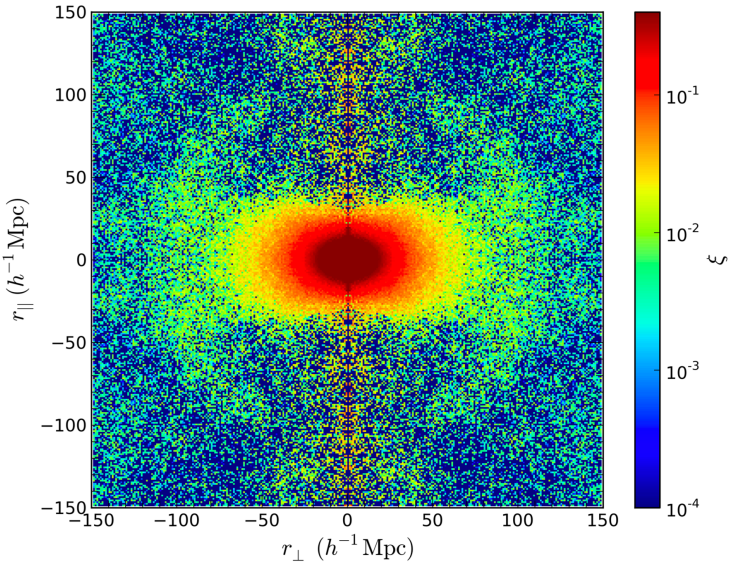

Figure 1: Two-dimensional correlation function measured from the BOSS galaxy sample, adapted from Ref. [5].

Kaiser formula

(Kaiser, 1987, MNRAS, 227, 1)

- Mass conservation $(1+\delta^r)\,d^3r = (1+\delta^s)\,d^3s$
- Jacobian $\dfrac{d^3s}{d^3r} = \left(1+\dfrac{v}{z}\right)^2 \left(1+\dfrac{dv}{dz}\right)$
- Distant observer $1+\delta^s = (1+\delta^r)\left(1+\dfrac{dv}{dz}\right)^{-1}$
- Potential flow $\dfrac{dv}{dz} = -\dfrac{d^2}{dz^2}\nabla^{-2}\theta$
- Proportionality $\delta^s(\mathbf{k}) = \delta^r(\mathbf{k}) + \mu_k^2\theta(\mathbf{k}) \simeq \left(1+f\mu_k^2\right)\delta^r(\mathbf{k})$

Figure 2: Schematic illustration of the linear Kaiser effect. In real space the clustering pattern is isotropic, while in redshift space coherent infall enhances the apparent clustering anisotropy along the line of sight.

9.4 Detailed AP mapping

The AP effect is a geometric anisotropy caused by adopting an incorrect fiducial cosmology when converting angles and redshifts to distances [1]. The scaling parameters are

$$\alpha_\parallel = \frac{H^{\rm fid}(z)\, r_s^{\rm fid}(z_d)}{H(z)\, r_s(z_d)}, \qquad \alpha_\perp = \frac{D_A(z)\, r_s^{\rm fid}(z_d)}{D_A^{\rm fid}(z)\, r_s(z_d)}.$$

Writing the coordinate transformation as

$$\mathbf{x}' = S \cdot \mathbf{x}, \qquad \mathbf{k}' = S^{-1} \cdot \mathbf{k},$$

with

$$S = \begin{pmatrix} \alpha_\perp^{-1} & 0 & 0 \\ 0 & \alpha_\perp^{-1} & 0 \\ 0 & 0 & \alpha_\parallel^{-1} \end{pmatrix},$$

one obtains

$$P'(\mathbf{k}') = |S|\, P(S \cdot \mathbf{k}'),$$

which can be written explicitly as

$$P'(k'_\parallel, \mathbf{k}'_\perp) = \frac{1}{\alpha_\perp^2 \alpha_\parallel} P\left(\frac{k'_\parallel}{\alpha_\parallel}, \frac{\mathbf{k}'_\perp}{\alpha_\perp}\right).$$

If the underlying anisotropy is modeled by linear RSD together with a Lorentzian small-scale damping term, then

$$P(k_\parallel, \mathbf{k}_\perp) = P_0(k)(1+\beta\mu^2)^2 D(k\mu\sigma_p) = P_0(k) k^{-4} \left[k_\perp^2 + (\beta+1)k_\parallel^2\right]^2 D(k_\parallel \sigma_p),$$

where

$$D(k'\mu'\sigma'_p) = \frac{1}{1 + (k'\mu'\sigma'_p)^2/2}.$$

Then

$$P'(\mathbf{k}') = \frac{1}{\alpha_\perp^2 \alpha_\parallel} P_0\left(\sqrt{\frac{k_\perp'^2}{\alpha_\perp^2} + \frac{k_\parallel'^2}{\alpha_\parallel^2}}\right) \left(\frac{k_\perp'^2}{\alpha_\perp^2} + \frac{k_\parallel'^2}{\alpha_\parallel^2}\right)^{-2} \times \left[\frac{k_\perp'^2}{\alpha_\perp^2} + (\beta+1)\frac{k_\parallel'^2}{\alpha_\parallel^2}\right]^2 D\left(\frac{k'_\parallel \sigma_p}{\alpha_\parallel}\right).$$

Defining $F \equiv \alpha_\parallel / \alpha_\perp$, one may also write

$$P'(\mathbf{k}') = \frac{1}{\alpha_\perp^2 \alpha_\parallel} P_0\left[\frac{k'}{\alpha_\perp}\sqrt{1 + \mu'^2\left(\frac{1}{F^2} - 1\right)}\right] \times \left[1 + \mu'^2\left(\frac{1}{F^2} - 1\right)\right]^{-2} \left[1 + \mu'^2\left(\frac{\beta+1}{F^2} - 1\right)\right]^2 D(k'\mu'\sigma'_p).$$

The transformed variables are

$$k' = \frac{k}{\alpha_\perp}\left[1 + \mu^2\left(\frac{1}{F^2} - 1\right)\right]^{1/2},$$
$$\mu' = \frac{\mu}{F}\left[1 + \mu^2\left(\frac{1}{F^2} - 1\right)\right]^{-1/2}.$$

For power-spectrum multipoles,

$$P_\ell(k) = \left(\frac{r_s^{\rm fid}}{r_s}\right)^3 \frac{2\ell+1}{2\alpha_\perp^2 \alpha_\parallel} \int_{-1}^{1} {\rm d}\mu\, P_g\big[k'(k,\mu), \mu'(\mu)\big]\, \mathcal{L}_\ell(\mu),$$

which is the form commonly used in anisotropic BAO and RSD analyses [2].

References

References

[1] C. Alcock and B. Paczynski, "An evolution free test for non-zero cosmological constant," Nature **281**, 358 (1979).

[2] W. E. Ballinger, J. A. Peacock and A. F. Heavens, "Measuring the cosmological constant with redshift surveys," Mon. Not. Roy. Astron. Soc. **282**, 877 (1996), [astro-ph/9605017].

[3] N. Kaiser, "Clustering in real space and in redshift space," Mon. Not. Roy. Astron. Soc. **227**, 1 (1987).

[4] J. A. Peacock *et al.*, "A Measurement of the cosmological mass density from clustering in the 2dF Galaxy Redshift Survey," Nature **410**, 169 (2001), [astro-ph/0103143].

[5] L. Samushia *et al.*, "The clustering of galaxies in the SDSS-III Baryon Oscillation Spectroscopic Survey: measuring growth rate and geometry with anisotropic clustering," Mon. Not. Roy. Astron. Soc. **439**, 3504 (2014), [arXiv:1312.4899].

10 Summary

The main lesson of this lecture is that anisotropy in galaxy clustering has multiple causes. Coherent velocities produce the Kaiser effect, random halo motions produce Fingers-of-God, and an incorrect fiducial cosmology produces AP distortion. Modern survey analyses extract all of this information at once.

Suggested reading

- Kaiser (1987) for the linear RSD formula.
- Dodelson and Schmidt, chapter on large-scale structure.
- Review papers on anisotropic BAO and RSD analyses.

Homework

1. **Real to redshift space.** Starting from

$$\mathbf{s} = \mathbf{r} + \frac{v_\parallel}{aH}\hat{\mathbf{n}},$$

   explain why only the line-of-sight coordinate is distorted.

2. **Kaiser derivation.** Starting from

$$\delta_g^s(\mathbf{k}) = b(1+\beta\mu^2)\delta_m(\mathbf{k}),$$

   derive

$$P_g^s(k,\mu) = b^2(1+\beta\mu^2)^2 P_m(k).$$

3. **Multipole coefficients.** Using the Kaiser formula, show that the monopole coefficient is

$$1 + \frac{2\beta}{3} + \frac{\beta^2}{5}.$$

You may use the integrals

$$\int_{-1}^{1} \mu^2 \, \mathrm{d}\mu = \frac{2}{3}, \qquad \int_{-1}^{1} \mu^4 \, \mathrm{d}\mu = \frac{2}{5}.$$

4. **AP scaling.** If $\alpha_\perp = 1.03$ and $\alpha_\parallel = 0.97$, explain whether radial scales are inferred to be too large or too small in the fiducial cosmology.

5. **Kaiser versus Fingers-of-God.** In one page or less, compare the physical origin of the large-scale Kaiser effect and the small-scale Fingers-of-God effect.

6. **Optional coding task.** Plot the Kaiser anisotropy factor $(1 + \beta\mu^2)^2$ as a function of μ for $\beta = 0.2$, 0.4, and 0.8.